133 (1975); B. A. Mamyrin, I. N. Tolstikhin, G. S. Anufriev, I. L. Kamanskiy, *Dokl. Akad. Nauk SSSR* **184**, 1197 (1969); W. B. Clarke, M. A. Beg, H. Craig, *Earth Planet. Sci. Lett.* **6**, 213 (1969).
3. L. H. Kellogg and G. J. Wasserburg, *Earth Planet. Sci. Lett.* **99**, 276 (1990).
4. C. J. Allègre, T. Staudacher, P. Sarda, *ibid.* **81**, 127 (1986).
5. R. K. O'Nions and I. N. Tolstikhin, *ibid.* **124**, 131 (1994).
6. D. Porcelli and G. J. Wasserburg, *Geochim. Cosmochim. Acta* **59**, 4921 (1995).
7. B. Marty, *Earth Planet. Sci. Lett.* **94**, 45 (1989).
8. ——— and P. Allé, in *Noble Gas Geochemistry and Cosmochemistry*, J. Matsuda, Ed. (Terra Scientific, Tokyo, 1994), pp. 191–204.
9. M. D. Kurz, W. J. Jenkins, S. R. Hart, D. Clague, *Earth Planet. Sci. Lett.* **66**, 388 (1983).
10. G. W. Wetherill, *Phys. Rev.* **96**, 679 (1954).
11. M. Honda, I. McDougall, D. Patterson, A. Doulgeris, D. Clague, *Nature* **349**, 149 (1991); P. Sarda, T. Staudacher, C. J. Allègre, *Earth Planet. Sci. Lett.* **91**, 73 (1988).
12. R. Poreda and K. Farley, *Earth Planet. Sci. Lett.* **113**, 129 (1992).
13. T. Staudacher *et al.*, *ibid.* **96**, 119 (1989).
14. D. E. Fisher, *ibid.* **123**, 199 (1994).
15. F. Pineau and M. Javoy, *ibid.*, p. 179.
16. M. Javoy and F. Pineau, *ibid.* **107**, 598 (1991).
17. P. H. Sarda and D. Graham, *ibid.* **97**, 268 (1990); D. Graham and P. Sarda, *ibid.* **105**, 568 (1991).
18. The analytical technique used is slightly modified from (*25*). Thick sections (~300 μm) were thoroughly cleaned and loaded into an ultra high–vacuum chamber with glass viewports. Selected vesicles were lasered with short (<0.5 s) pulses using a continuous wave (CW) yttrium-aluminum-garnet-Nd (YAG Nd) laser (~3 W power; beam diameter < 100 μm). The pressure increase resulting from gas released from the vesicles was measured by capacitance manometer (MKS Baratron) within a calibrated volume (0.2 liter). A small sample (~5%) was abstracted and analyzed for major gas (CO_2, H_2O, N_2, and CH_4) composition. The remaining gas was purified (using two SAES NP10 getters) and separated into He and Ar fractions with liquid N_2–cooled activated charcoal, and these fractions were subsequently analyzed with a VG5400 noble gas mass spectrometer. Procedural blanks were continually monitored (on average, three blanks were performed per analysis) and maintained at very low and consistent levels by careful vacuum practice. The total variation in ^{36}Ar blank (2σ) during the 6-week analysis period was 1.5×10^{-13} cm^3 STP with variations on a day-to-day basis of 0.8×10^{-13} cm^3 STP; typical blank levels were $<6 \times 10^{-13}$ cm^3 STP. All ^{36}Ar analyses presented here are 2σ or more above the blank, not lower limits calculated with the system detection capabilities. ^{40}Ar and ^4He blanks do not affect the data (<1% of a typical sample).
19. M. Y. Spasneykhh and I. N. Tolstikhin, *Geochem. J.* **27**, 213 (1993).
20. M. R. Carroll and E. M. Stolper, *Geochim. Cosmochim. Acta* **57**, 5039 (1993).
21. K. P. Jochum, A. W. Hofmann, E. Ito, H. M. Seufert, W. M. White, *Nature* **306**, 431 (1983).
22. R. K. O'Nions and D. McKenzie, *Philos. Trans. R. Soc. London Ser. A* **342**, 65 (1995).
23. D. Phinney, J. Tennyson, U. Frick, *J. Geophys. Res.* **83**, 2313 (1978).
24. K. A. Farley and H. Craig, *Geochim. Cosmochim. Acta* **58**, 2509 (1994).
25. P. G. Burnard, F. M. Stuart, G. Turner, *Earth Planet. Sci. Lett.* **128**, 243 (1994).
26. D. B. Patterson, M. Honda, I. McDougall, *Geophys. Res. Lett.* **17**, 705 (1990).
27. Radiogenic and nucleogenic production of ^{20}Ne and ^{22}Ne within the mantle is negligible, therefore the mantle $^{20}Ne/^{22}Ne$ ratio is related to the primordial (that is, trapped during accretion) Ne isotope composition. Mantle samples have $^{20}Ne/^{22}Ne$ ratios up to ~13 (*11*), distinct from the atmospheric value of 9.8. Solar $^{20}Ne/^{22}Ne$ ratios are between 13.3 and 13.8 (*30*), consistent with solar Ne trapped in the mantle.
28. D. M. Hunten, R. O. Pepin, J. C. B. Walker, *Icarus* **69**, 532 (1987).
29. T. Owen, A. Bar-Nun, I. Kleinfield, *Nature* **358**, 43 (1992).
30. A. Pedroni and F. Begeman, *Meteoritics* **29**, 632 (1994); J.-P. Benkert, H. Baur, P. Signer, R. Wieler, *J. Geophys. Res.* **98**, 13 (1993); R. Wieler and H. Baur, *Meteoritics* **29**, 570 (1992); R. H. Becker and R. O. Pepin, *Earth Planet. Sci. Lett.* **103**, 55 (1991); R. Wieler, H. Baur, P. Signer, *Geochim. Cosmochim. Acta* **50**, 1997 (1986).
31. T. Swindle, in *Meteorites and the Early Solar System*, J. F. Kerridge and M. S. Matthews, Eds. (Univ. of Arizona Press, Tucson, 1988), pp. 535–564.
32. The calculated production of ^{40}Ar and ^4He in the lower mantle (lm) is 5.7 and 10×10^{14} atoms g^{-1}, respectively (*6*). Assuming $^4He/^3He_{lm} = 20{,}000$, then $[^3He]_{lm} = 10 \times 10^{14}/20{,}000 = 5 \times 10^{10}$ atoms g^{-1}. If the mantle trapped solar He and Ar relative abundances, then $^3He/^{36}Ar_{lm} = 12$ to 15, $[^{36}Ar]_{lm} = [^3He]_{lm}/12 = 4.2 \times 10^9$ to 3.3×10^9 atoms g^{-1} and $^{40}Ar/^{36}Ar = 135{,}000$ to 171,000.
33. C. L. Harper Jr. and S. B. Jacobsen, *Science* **273**, 1814 (1996).
34. G. W. Wetherill, *ibid.* **228**, 877 (1985); H. J. Melosh, *Impact Cratering: A Geologic Process*, vol. 11 of *Oxford Monographs on Geology and Geophysics*, H. Charnock *et al.*, Eds. (Oxford Univ. Press, Oxford, 1989).
35. R. K. O'Nions and I. N. Tolstikhin, *Earth Planet. Sci. Lett.* **139**, 213 (1996).
36. Supported by the Natural Environment Research Council BRIDGE initiative (grant GST/02/1139). Thanks to T. Glenn for technical wizardry. The manuscript was considerably improved by the comments of two anonymous reviewers.

16 December 1996; accepted 20 February 1997

Climatic Limits on Landscape Development in the Northwestern Himalaya

Nicholas Brozović,*† Douglas W. Burbank, Andrew J. Meigs‡

The interaction between tectonism and erosion produces rugged landscapes in actively deforming regions. In the northwestern Himalaya, the form of the landscape was found to be largely independent of exhumation rates, but regional trends in mean and modal elevations, hypsometry (frequency distribution of altitude), and slope distributions were correlated with the extent of glaciation. These observations imply that in mountain belts that intersect the snowline, glacial and periglacial processes place an upper limit on altitude, relief, and the development of topography irrespective of the rate of tectonic processes operating.

On scales of years to thousands of years, mountains are generally viewed as approximately static masses of rock whose surfaces are etched by erosion (*1*). In contrast, on scales of tens of thousands to millions of years, tectonic and geomorphic processes may lead to the exhumation of rocks once buried tens of kilometers in the crust (*2*). Typically the presence of elevated topography has been interpreted as a response to enhanced rates of rock uplift, whereas apparent altitudinal limits to topography have been interpreted in terms of rock strength or gravitational collapse (*3–5*). Here, we compared indices of exhumation and geomorphic and climatic data with digital topographic analysis and found that in the actively deforming northwestern Himalaya, climate is the fundamental control on the development of topography.

Our study area covered more than 40,000 km^2 of the northwestern Himalaya and Karakoram (Fig. 1). The juxtaposition of deeply incised river gorges and mountain peaks forms the world's largest, steepest terrestrial relief: in less than 30 km the elevation drops from 8125 and 7788 m at the summits of Nanga Parbat and Rakaposhi, respectively, to about 1500 m in the Indus and Hunza valleys. This relief creates an altitudinal zonation of climatic, ecologic, and geomorphic regimes (*6*, *7*). Much of the landscape is dominated by glacial and periglacial processes, and a southwest-to-northeast gradient of decreasing annual precipitation controls the lower altitudinal limit of permanent snow (the snowline) and the extent of glaciation (*6–8*). Sediment yield, bedrock incision, and historic landslide data (*9*, *10*) indicate that modern-day erosion rates are uncommonly high (up to 12 mm/year along the middle Indus gorge).

On the basis of relief and degree of dissection, we divided our study area into eight distinct physiographic regions consisting of undissected plateaus, dissected plateaus, and deeply incised mountainous regions (Fig. 2A). Each region has an area of several thousand square kilometers, and the boundaries between regions were taken either at the mid-points of major valleys or along major faults or structural trends. We used a 90-m grid space digital elevation model

Department of Earth Sciences, University of Southern California, Los Angeles, CA 90089, USA.

*Present address: Department of Geology and Geophysics, University of California, Berkeley, CA 94720, USA. E-mail: nick@moray.berkeley.edu
†To whom correspondence should be addressed.
‡Present address: Division of Geological and Planetary Sciences, California Institute of Technology, Pasadena, CA 91125, USA.

(DEM) (*11*) to calculate the hypsometry (the relation between area and altitude) and slope distributions as a function of altitude within the eight regions (Figs. 2 and 3).

Almost half of the land area lies between 4000- and 5000-m altitude, which represents only 12% of the total relief (Fig. 3). Four-fifths of the area lies within less than half of the relief (3000 to 6000 m). Although there are many peaks higher than 7000 m, only ~1% of the area lies above 6000 m. Even though relief in the subregions varies from 1500 m to more than 7000 m, the modal elevation (the elevation with the greatest frequency in the landscape) is between 4000 and 5000 m in all cases, irrespective of whether the regions are undissected plateaus (the Deosai Plateau), partially dissected plateaus (the Gamugah surface, parts of the Deosai Plateau, and the Ghujerab mountains), or deeply dissected mountainous regions (Nanga Parbat, Haramosh and Rakaposhi, and the Karakoram). Mean elevations vary between ~3200 m for the Gamugah surface and ~4800 m for the Ghujerab mountains (Fig. 2A) and generally increase to the north and east of the study area. The mean elevation of the Nanga Parbat region (~3800 m), which contains the highest peak in the study area (8125 m) and one of the highest peaks in the world (*12*), is lower than the means of both the adjacent dissected portion of the Deosai Plateau (~4100 m) and the entire data set (~4200 m).

To constrain landform variability with altitude, we subdivided the landscape into 500-m vertical bins and analyzed the slope distributions for each bin for the eight regions (*13*). Slope angles in all the regions analyzed except the undissected portion of the Deosai Plateau vary similarly with altitude (Fig. 3). They display steep slopes at high altitudes (>5500 m), gentler slopes at low altitudes (<4000 m), and a local minimum in slope from 4000 to 5000 m (an elevation near the modal elevation of each area). Areally extensive, gentle slopes are associated with the confluence of the Indus and Gilgit rivers, the Skardu Basin, and some of the larger Karakoram glaciers (Fig. 3). These areas are represented by spikes in the hypsometry and a depression of the 25th percentile of slope angles for the regions that contain them.

The large area that lies between 4000 and 5000 m might be interpreted as the remnants of an erosion surface or plateau. Several planation surfaces have been identified in the northwestern Himalaya (*14*), but these are of limited areal extent and have low slope angles. In contrast, the region between 4000 and 5000 m is large (45% of the area) and has an average slope of about 25° (Fig. 3). Thermochronologic data from the northwestern Himalaya and Karakoram show that a large part of the region has undergone many kilometers of exhumation during the last several million years (*10, 15*). Spatially this exhumation has been highly variable (Fig. 1) and locally rapid, reaching 5 km/My along the Nanga Parbat–Haramosh axis (*15*). Thus, any surfaces of late Tertiary age would have been eroded from most of the study area; the region of less steep slopes that lies between 4000 and 5000 m cannot represent remnants of an erosion surface (such as an extension of the Tibetan Plateau).

Though the study area encompasses several distinct lithological sequences (*2*), trends of slope angles with altitude are regionally consistent and unrelated to these lithological variations. Hence, rock properties cannot be the only control on hillslope development in the northwestern Himalaya. Because there is a local minimum in slopes around 4000 m, slope angles are not a linear function of altitude, as has been suggested (*7*). Although the slope minimum between 4000 and 6000 m cannot be ascribed solely to a change from fluvially incised V-shaped valley profiles to glacially incised U-shaped valley profiles (*16*), it follows trends in the altitude of the snowline, rising to the north and east (Fig. 2B). We speculate that the moderation of slopes observed in the northwestern Himalaya is caused by extensive glacial scouring of the landscape coupled with vigorous freeze-thaw action, which is most effective between 4000 and 6000 m because of abundant moisture (*7*). The consistent relation between modal elevation, slope distributions, and the altitude of the snowline across regions that are undergoing exhumation at very different rates (Figs. 1 and 3) leads us to conclude that climate is the ultimate control on large-scale landscape development in the region.

In considering the importance of glaciation on a landscape over geological time scales, it is critical to realize that we are

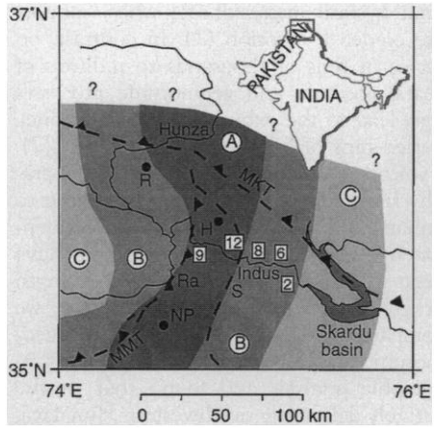

Fig. 1. Location map of the western syntaxis of the Himalaya, showing major peaks and rivers, trends in apatite fission-track cooling ages (*15*), and representative cosmogenic nuclide incision rates (*10*). NP, Nanga Parbat (8125 m); H, Haramosh (7397 m); R, Rakaposhi (7788 m). Apatite fission-track cooling age zones: A, 0 to 1 million years (My); B, 1 to 6 My; C, 6 to 15 My. Ra, Raikot fault; S, Stak fault; MMT, Main Mantle Thrust; MKT, Main Karakoram Thrust. Fluvial incision rates inferred from cosmogenic nuclide ages for the Indus River (*10*) are shown in boxes, with units of millimeters per year, equivalent to kilometers per million years.

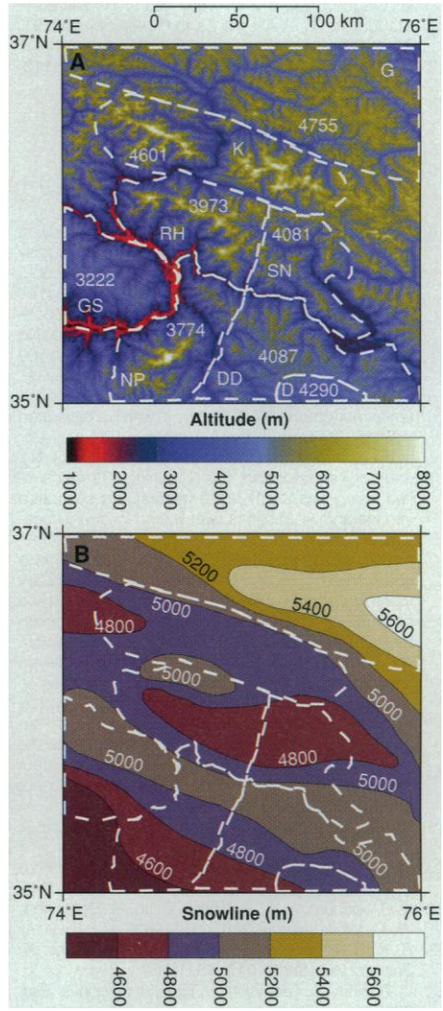

Fig. 2. (**A**) Map showing 1-km digital topography of the study region and the physiographic areas used in the analysis. The area corresponds to that shown in Fig. 1. The 90-m DEM we used in the analysis has a resolution about 100 times better than this image (*11*). NP, Nanga Parbat; D, Deosai Plateau (undissected); DD, dissected portion of Deosai Plateau; GS, Gamugah surface; RH, Rakaposhi and Haramosh; SN, area north of Skardu Basin; K, western Karakoram; G, Ghujerab mountains (northern Karakoram). Mean elevations for each subregion are shown. (**B**) Snowline altitudes for the study region (*8*).

presently in an interglacial period, and that both full-glacial and average Quaternary climatic conditions entailed more extensive glaciation (*17*). A common measure of the extent of glaciation is the equilibrium line altitude (ELA), the altitude on a glacier at which annual accumulation is exactly matched by annual ablation, so that the net mass balance for the glacier is zero. We used regional snowlines (*8*) as both a general climatic indicator and a proxy for regional ELAs for three reasons. First, ELAs are significantly affected by microclimate and minor topographic variations (*18*), whereas we were concerned with regional trends. Second, many glaciers in the northwestern Himalaya are fed by avalanches (*7, 19*), and large portions of their contributing areas are unglaciated, making ELA calculation from topographic maps difficult. Third, the inaccessibility of the region has meant that there are few studies that have measured ELAs in the field, and these have been limited to the main valleys (*19–21*). Where several studies have concentrated on the same glacier, ELA measurements often show significant variations (*19–21*).

Hypsometry places an important control on glacier mass balance during climatic fluctuations (*22*). When the ELA is dropping, the rate at which the extent of glaciated terrain in the landscape increases depends on hypsometry: Small changes in ELA significantly increase the percent surface area covered by glaciers when the region lies at an altitude similar to the ELA. In the northwestern Himalaya, ELAs during the last glacial maximum (LGM) are estimated to have been between 600 and 1000 m lower than at present (*18*). The long-term mean position of ELAs during the Quaternary is estimated to have been ~400 to 500 m lower (*17*). Using the hypsometry, we calculated the changes in surface area above the snowline that would result in the study regions for a given lowering or raising of the ELA (Fig. 4); this change in area is related to the total glacier accumulation area. For the deeply incised mountainous regions (Nanga Parbat, the Karakoram, and Haramosh and Rakaposhi), there is an approximately linear relation between ELA lowering and the area above the snowline (Fig. 4). Modern-day glaciers in the Karakoram are extensive (*8, 19*); conditions at the LGM would have nearly doubled the area above the snowline available for their accumulation areas. For the Nanga Parbat and Haramosh and Rakaposhi regions, LGM conditions could have nearly quadrupled the area above the snowline, and average Quaternary conditions would have doubled the area. For the plateaus and dissected plateaus, the effect of lowering ELAs is even greater on the landscape (Fig. 4): The Deosai Plateau is unglaciated today but would have been blanketed by an ice sheet during LGM conditions.

We suggest that the hypsometric configuration found in the northwestern Himalaya is stabilized through the operation of two separate negative feedback mechanisms: hypsometric forcing of glaciers and

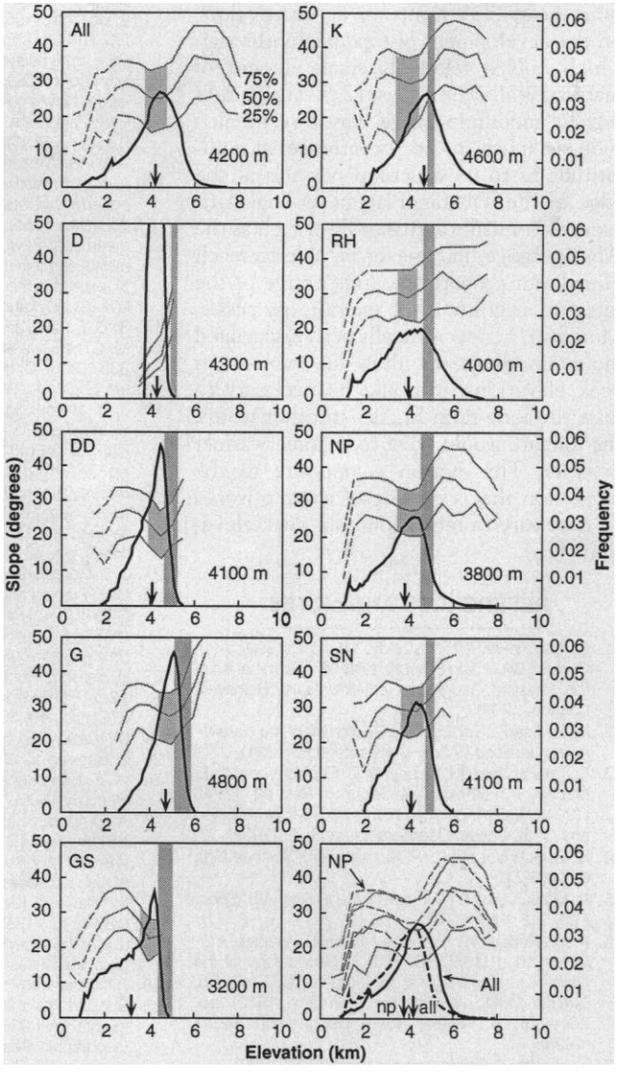

Fig. 3. Landscape analysis for the regions shown in Fig. 2. The abbreviations are the same as for Fig. 2, and "All" is the entire data set. The thick black line on each graph is the hypsometry (frequency distribution of altitude) for that region. The frequency data have been binned in 100-m vertical intervals and normalized to allow direct comparison between regions with different areas. The arrows on the horizontal axes indicate the mean elevation for each region; values are inside the graphs. The vertical dark gray lines running from top to bottom in the graphs show the range of snowline altitudes for each region, from Fig. 2B. The three subhorizontal gray lines show the 25th, 50th, and 75th percentile of slope distributions as a function of altitude, calculated with 500-m vertical bins (*13*). The light gray shaded areas on the slope distribution curves highlight the regions of moderated slopes that generally coincide with modal elevations. On several of the slope distribution curves, the lowermost several hundred meters are dotted: these lower slopes result from sampling of the wider valley floors of the Indus and Hunza rivers and do not reflect a rapid increase of slope with altitude. The bottom right-hand graph shows the similarity between data for the Nanga Parbat region, thought to be undergoing denudation of between 5 and 10 km/My (*10, 15*), and the entire data set. The arrows labeled "np" and "All" on the horizontal axis indicate the mean elevations of the Nanga Parbat data and the entire data set, respectively.

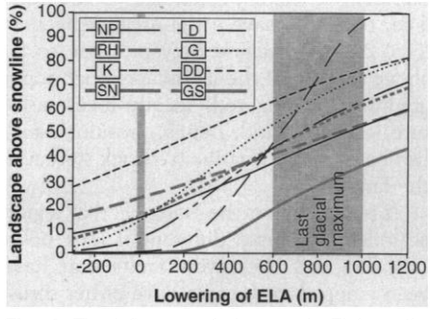

Fig. 4. The influence of changes in ELA on the extent of terrain above the snowline. Portions of the hypsometry for the regions of Fig. 2 are integrated to show the percentage of the area above the snowline for various changes in the ELA. The vertical gray lines denote present-day conditions and the range of last glacial maximum conditions (*18*). As an example, for the Rakaposhi and Haramosh region, a lowering of the ELA by 600 m will double the area above the snowline. Because the slope of the integrated Rakaposhi and Haramosh hypsometric curve is the lowest of all the regions analyzed, it shows the smallest magnitude of response to changes in ELA. The other regions will show larger responses to ELA changes, proportional to their slopes.

topographic lightning rods (features considerably higher than the surrounding landscape). Changes in the ELA affect the size of the glacial accumulation area as a direct function of landscape hypsometry (*22*). Any surface uplift (whether isostatically or tectonically driven) represents a relative lowering of ELA within the landscape, so that surface uplift and rock uplift in the absence of erosion will tend to cause an increase in the glacier-covered area. Increasing glacier accumulation areas will also increase ice flux, and it is argued that this will increase erosion rates (*23*), thus returning the landscape toward its previous hypsometry. On the north slope of Nanga Parbat, modern-day denudation is 4.6 to 6.9 mm/year for the glaciated area and 1.4 to 2.1 mm/year for the unglaciated part of the basin (*21*). If these erosion rates are maintained during an increase in accumulation area, the basin-wide erosion rate will increase rapidly during lowering of the ELA.

Although the three highly incised mountainous regions have mean elevations similar to those of the undissected plateaus, their maximum elevations are significantly higher (Fig. 3). These regions (Nanga Parbat, Haramosh and Rakaposhi, and the Karakoram) have a small amount of land (1 to 2%) at high elevations (>6500 m). We suggest that these peaks are remnants of topography that surface processes have not quite managed to remove, whose maximum relief is determined by rock strength (*4*). Such regions are characterized by steep slopes, often too steep and cold to be glaciated (*7, 24*). Even though these regions represent a small percentage of the total area, they will have a significant effect on local climate because they protrude so far above the rest of the landscape. Such topographic lightning rods locally focus moisture (*25*), ice, and, hence, erosion, establishing another negative feedback system in the landscape.

It is argued that the Nanga Parbat region is undergoing rapid differential rock uplift (*10, 15*). All the active faults that have been mapped in the area have either thrust or strike-slip displacements; no major active normal faults have been documented (*2, 15*). Nevertheless, the mean elevations in this region of active deformation (3200 to 4800 m) are all less than that of the Tibetan Plateau, for which the mean elevation is ~5000 m (*11*). In Tibet, snowline altitudes are as high as 6400 m, and only a small area is presently glaciated (*8, 19*). Active normal faulting is interpreted to be a result of gravitational collapse of the plateau (*5*). In contrast to Tibet, we suggest that in the northwestern Himalaya, the efficiency of surface processes (and, in particular, glaciation) has prevented the mountain range from reaching mean elevations at which the driving forces of tectonism could no longer support it. However, the topographic controls imposed by glaciation are insensitive to the cause of rock uplift, so that both tectonically and isostatically driven rock uplift would result in similar appearing landscapes. It is impossible to differentiate isostatic and tectonic components of rock uplift within continental orogenic systems such as the Himalaya purely from a surface perspective; constraints on the rates of crustal-scale processes are needed.

These Himalayan data suggest that the height attained by a mountain belt with abundant precipitation once it is extensively glaciated is a function of the ELA rather than of rock uplift rates. Maximum and mean mountain elevations generally decrease as a function of increasing latitude and decreasing ELA (*26*). Thus, the long-term mean ELA forms an upper envelope on the development of topography through which only a relatively small amount of material is allowed to pass (*27*). The world's highest mountain range may owe its altitude as much to its occurrence at mid-latitude as to its structural position at the edge of the Tibetan Plateau. A high-latitude, tectonically active orogen, such as the Alaska Range, may never be able to reach Himalayan proportions, irrespective of the rates or magnitudes of tectonic processes. Moreover, in a tectonically active, glaciated mountain range, to allow an increase in peak elevations, it would be necessary to raise the long-term ELAs—in other words, the climate would have to become warmer or drier. This notion is opposite to the suggestion that a cooling of climate would be necessary to raise mountain peak elevations (*28*).

REFERENCES AND NOTES

1. O. Slaymaker, *Mt. Res. Dev.* **10**, 171 (1990); A. J. Gerrard, *Mountain Environments: An Examination of the Physical Geography of Mountains* (Belhaven, London, 1990).
2. M. P. Searle, *Geology and Tectonics of the Karakoram Mountains* (Wiley, Chichester, UK, 1991).
3. For example, H. M. Kelsey, D. C. Engebretson, C. E. Mitchell, R. L. Ticknor, *J. Geophys. Res.* **99**, 12245 (1994); R. S. Anderson, *ibid.*, p. 20161; N. A. Lifton and C. G. Chase, *Geomorphology* **5**, 77 (1992).
4. K. M. Schmidt and D. R. Montgomery, *Science* **270**, 617 (1995).
5. P. Molnar and H. Lyon-Caen, *Geol. Soc. Am. Spec. Pap.* **218**, 179 (1988).
6. K. H. Paffen, W. Pillewizer, H. J. Schneider, *Erdkunde* **10**, 1 (1956); C. Troll, in *Geoecology of the High Mountain Regions of Eurasia*, C. Troll, Ed. (Steiner Verlag, Wiesbaden, Germany, 1972), pp. 264–275; S. Weiers, *Bonn. Geogr. Abh.* **92**, 1 (1995).
7. K. Hewitt, *Z. Geomorphol. Suppl.* **76**, 9 (1989).
8. H. von Wissmann, *Akad. Wiss. Lit. Mainz Abh. Math. Naturwiss. Kl. Jahrg.* **14**, 4 (1959).
9. R. I. Ferguson, in *International Karakoram Project*, K. Miller, Ed. (Cambridge Univ. Press, Cambridge, 1984), vol. 2, pp. 581–598; K. Hewitt, *Science* **242**, 64 (1988); J. F. Shroder Jr., in *Himalaya to the Sea: Geology, Geomorphology and the Quaternary*, J. F. Shroder Jr., Ed. (Routledge, New York, 1993), pp. 1–42.
10. D. W. Burbank *et al.*, *Nature* **379**, 505 (1996).
11. E. J. Fielding, B. L. Isacks, M. Barazangi, C. Duncan, *Geology* **22**, 163 (1994).
12. Although incision along the Indus and Astor rivers does lower the mean elevation in the Nanga Parbat region, this effect is relatively small, and the calculated mean varies little for regional boundaries which are taken well outside of the immediate influence of the deeply incised gorges of these rivers.
13. Slope angles are sensitive to both DEM grid spacing and to the length scale over which slope is measured, and in general, slope angles decrease with increasing measurement length. We calculated mean slope angles by fitting a least square deviation best fit plane to groups of four-by-four pixels, corresponding to ~270 m by 270 m on the ground (*10, 11*). For the 90-m DEM, slope angles will be underestimated by this technique, but multiple hillslopes will generally not be averaged into one calculation (*11*). Thus, we place more significance on trends in slope angles than on their absolute values.
14. E. Derbyshire, L. Jijun, F. A. Perrott, X. Shuying, R. S. Waters, in *International Karakoram Project*, K. Miller, Ed. (Cambridge Univ. Press, Cambridge, 1984), vol. 2, pp. 456–495; L. A. Owen, *Tectonophysics* **163**, 227 (1989); J. F. Shroder Jr., L. A. Owen, E. Derbyshire, in *Himalaya to the Sea: Geology, Geomorphology and the Quaternary*, J. F. Shroder Jr., Ed. (Routledge, New York, 1993), pp. 132–158.
15. P. K. Zeitler *et al.*, *Geol. Soc. Am. Spec. Pap.* **232**, 1 (1989); D. M. Winslow, P. K. Zeitler, C. P. Chamberlain, I. S. Williams, *Tectonics* **15**, 1292 (1996).
16. A shift toward a bimodal slope distribution composed of oversteepened valley sides and gently sloping valley floors in glaciated areas might lower the mean, but it would also increase the interquartile range, and this trend is not observed in the data (Fig. 3), except in the Karakoram where major glacial valleys do produce spikes in the slope distribution.
17. S. C. Porter, *Quat. Res.* **32**, 245 (1989).
18. M. C. Sharma and L. A. Owen, *Quat. Sci. Rev.* **15**, 335 (1996); C. H. Scott, thesis, University of Leicester, England (1992).
19. J. H. Mercer, in *Mountain Glaciers of the Northern Hemisphere*, W. O. Field, Ed. (American Geographical Society of New York, New York, 1975), vol. 1, pp. 371–409.
20. See reviews in (*19*) and in J. A. Holmes, in *Himalaya to the Sea: Geology, Geomorphology and the Quaternary*, J. F. Shroder Jr., Ed. (Routledge, New York, 1993), pp. 72–90.
21. J. S. Gardner and N. K. Jones, in *ibid.*, pp. 184–197.
22. D. J. Furbish and J. T. Andrews, *J. Glaciol.* **30**, 199 (1984); S. C. Porter, *Geol. Soc. Am. Bull.* **81**, 1421 (1970); M. Kuhle, *Geojournal* **17**, 545 (1988); E. E. Small, *Geomorphology* **14**, 109 (1995).
23. B. Hallet, L. Hunter, J. Bogen, *Global Planet. Change* **12**, 213 (1996); N. F. Humphrey and C. F. Raymond, *J. Glaciol.* **40**, 539 (1994).
24. M. Kuhle, *Geojournal*, **13**, 331 (1986).
25. Z. Benxing, *Z. Geomorph. Suppl.* **76**, 89 (1989).
26. W. S. Broecker and G. H. Denton, *Sci. Am.* **262**, 48 (January 1990).
27. A comparable idea put forward by A. Penck over a century ago [*Schr. Ver. Verbr. Naturwiss. Kennt. Wien* **27** (1886–87)] is that increasing frost intensity at high latitudes limits mountain heights. Similarly, G. M. Dawson [*Geol. Surv. Can. Annu. Rep. VII B* (1896), p. 11] suggested that higher erosion rates above the snowline lead to the "rapid disappearance of rock-masses above this height."
28. P. Molnar and P. England, *Nature* **346**, 29 (1990).

29. Support for this research was provided by NSF (grants EAR 9205501 and EAR 9220056), National Geographic Research, and NASA. We thank B. L. Isacks and E. J. Fielding for contributions to the DEM analysis, and two anonymous reviewers for their comments. The hospitality and support of the staff at Victoria University, Wellington, are also acknowledged.

17 December 1996; accepted 10 March 1997